Published in final edited form as:
Bioorg Med Chem Lett. 2011 July 15; 21(14): 4238–4242. doi:10.1016/j.bmcl.2011.05.078.

Small molecule inhibitors of SHP2 tyrosine phosphatase discovered by virtual screening

Zhi-Hong Yu[a], **Lan Chen**[a,b], **Li Wu**[a,b], **Sijiu Liu**[a], **Lina Wang**[a], and **Zhong-Yin Zhang**[a,b,*]

[a]Department of Biochemistry and Molecular Biology, Indiana University School of Medicine, 635 Barnhill Drive, Indianapolis, IN 46202, USA

[b]Chemical Genomics Core Facility, Indiana University School of Medicine, 635 Barnhill Drive, Indianapolis, IN 46202, USA

Abstract

SHP2, encoded by *PTPN11*, is a non-receptor protein tyrosine phosphatase (PTP) containing two tandem Src homology-2 (SH2) domains. It is expressed ubiquitously and plays critical roles in growth factor mediated processes, primarily by promoting the activation of the RAS/ERK signaling pathway. Genetic and biochemical studies have identified SHP2 as the first bona fide oncoprotein in the PTP superfamily, and a promising target for anti-cancer and anti-leukemia therapy. Here, we report a structure-based approach to identify SHP2 inhibitors with a novel scaffold. Through sequential virtual screenings and *in vitro* inhibition assays, a reversible competitive SHP2 inhibitor (**C21**) was identified. **C21** is structurally distinct from all known SHP2 inhibitors. Combining molecular dynamics simulation and binding free energy calculation, a most likely binding mode of **C21** with SHP2 is proposed, and further validated by site-directed mutagenesis and structure-activity relationship studies. This binding mode is consistent with the observed potency and specificity of **C21**, and reveals the molecular determinants for further optimization based on the new scaffold.

Keywords

SHP2 inhibitor; Protein tyrosine phosphatase (PTP); Virtual screening; Molecular dynamics simulation; Drug discovery

Protein tyrosine phosphatases (PTPs) play crucial roles in a variety of cellular processes, working in concert with protein tyrosine kinases (PTKs) to control the tyrosine phosphorylation level and regulate key signaling cascades.[1, 2] Aberrant tyrosine phosphorylation has been linked to the aetiology of several human diseases (such as cancer, diabetes, obesity, and autoimmune disorders), which makes PTKs and PTPs important therapeutic targets.[3–5] Although the PTPs are generally recognized as negative regulators of signaling cascades, increasing evidence suggest that some PTPs, such as SHP2, PTP1B, CDC25 and PRL3, can also potentiate signaling cascades and have oncogenic potentials.[5–8]

*Corresponding author. Tel.: +1-317-274-8025; fax: +1-317-274-4686; zyzhang@iupui.edu.

Supplementary Material

Supplementary materials associated with this article can be found in the online version.

Therefore these PTPs represent promising targets for anti-cancer therapy, and interest in developing specific PTP inhibitors has intensified in recent years.[8–11]

SHP2, encoded by *PTPN11*, is a non-receptor PTP containing two tandem Src homology-2 (SH2) domains, one catalytic domain and a C-terminal tail. SHP2 is a positive transducer of growth factor, cytokine, integrin, and hormone signaling pathways regulating a diverse array of processes such as cell proliferation, differentiation, adhesion, migration and apoptosis, due primarily to its ability to promote the activation of the RAS/ERK signaling pathway.[12–15] Germline mutations in SHP2 causing hyperactivation of its phosphatase activity (namely gain-of-function mutations) are associated with Noonan syndrome (~50%).[16–18] Somatic gain-of-function SHP2 mutations are linked to juvenile myelomonocytic leukemia (JMML, ~34%), myelodysplastic syndrome (~10%), acute lymphoid leukemia (ALL, ~7%), acute myeloid leukemia (AML, ~4%), adult AML (~6%), as well as solid tumors, such as lung adenocarcinoma, colon cancer, neuroblastoma, melanoma and hepatocellular carcinoma.[18–24] In addition, SHP2 is implicated in gastric ulcer and gastric carcinoma.[25] These genetic and biochemical evidence identify SHP2 as the first bona fide oncoprotein in the PTP superfamily, which makes it a prime target for anti-leukemia and anti-cancer therapy and draws increasing interests in the development of SHP2 inhibitors.[26–35] To date, all reported SHP2 inhibitors (Fig. S1, Supplementary Material) display similar micromolar-to-submicromolar *in vitro* inhibitory activity and most of them lack the selectivity required for mechanistic studies, possibly due to the highly conserved active site pocket shared by all PTPs.[36] Consequently, there is still a need to discover new SHP2 inhibitors with novel scaffold, increased potency, selectivity and *in vivo* activity.

In an effort to discover novel SHP2 inhibitors, we carried out high-throughput virtual screenings on two subsets of ZINC[37] database targeting the active pocket of SHP2 catalytic domain (PDBID: 3B7O[38]). The details of site definitions, structure preparations and screening procedures were described in the Supplementary Material. After the initial screening with DOCK6.2[39,40] and the secondary screening with AutoDock4.01,[41,42] the top-ranked 1,621 molecules with energy score less than −8.5 kcal/mol were selected for further analyses, such as consensus score evaluation, similarity analysis and visual inspection of binding mode. Finally, 35 compounds were purchased and their inhibitory activity against SHP2 was assessed at 50 μM concentration. 9 out of the 35 compounds showed more than 50% inhibition, and another 7 showed inhibition ranging from 30% to 50% (Table S1, Supplementary Material). These 16 compounds were further assayed for IC_{50} values, and three of them (namely **C18**, **C21** and **C30**) showed concentration-dependent inhibition, their structures and IC_{50} are listed in Table 1. Moreover, the IC_{50} of these three compounds against SHP1 and PTP1B were also determined. **C30** and **C18** had only moderate inhibitory activity against SHP2 but better inhibition against PTP1B and SHP1 (Table S2, Supplementary Material). Thus they were not pursued further.

Compound **C21**, ranked the 20th in the initial screening and the 1st in the secondary screening, inhibited SHP2 with an IC_{50} of 8.3 μM. **C21** is structurally distinct from all known SHP2 inhibitors. Like most known SHP2 inhibitor, **C21** did not exhibit significant selectivity for SHP2 over its close homolog SHP1 (IC_{50} = 14 μM, only 1.7-fold), but it showed considerable selectivity against PTP1B (IC_{50} = 118 μM, 14.2-fold). To explore the selectivity of **C21** more broadly, an additional panel of nine representative PTPs, including cytosolic PTPs (TC-PTP and LYP), the receptor-like PTPs (CD45, LAR and PTPα), the dual specificity phosphatases (VHR, VHX and Cdc14) and the low molecular weight PTP (LMW-PTP) were employed for inhibition assay. **C21** showed an IC_{50} greater than 100 μM against TC-PTP, CD45, LAR, VHX and LMW-PTP, and almost no inhibition at 100 μM against LYP, PTPα, VHR and Cdc14, indicating excellent selectivity of **C21** for SHP2 over the panel of PTPs.

Moreover, the mode of inhibition by **C21** against SHP2 was also determined through steady-state enzyme kinetic analysis. The results suggest a reversible and competitive pattern for SHP2 inhibition by **C21** with an inhibition constant (K_i) of 4.6 μM (Fig. 1). Since the virtual screening was carried out aiming at the catalytic pocket, it was quite reasonable that the identified **C21** occupies the active site and acts as a competitive inhibitor. Collectively, the biochemical assays confirmed **C21** as a novel SHP2 inhibitor with micromolar potency.

To define the binding mode between **C21** and SHP2, we performed molecular docking with AutoDock4.01. After multiple docking runs and cluster analysis of binding conformations, two possible binding modes with comparable calculated binding free energy (BFE) were found. In mode **I** (Fig. 2a, BFE = −11.08 kcal/mol), the pyrazoline carboxyl moiety in **C21** penetrates into the active site pocket and interacts with residues in the phosphate-binding loop (P-loop); the two sulfonic groups are located at the entrance of the active site and interact with two basic residues K364 and K366. In mode **II** (Fig. 2b, BFE = −10.22 kcal/mol), **C21** binds almost at the same position but with completely opposite orientation: the benzene ring with two sulfonic groups wedge into the active site pocket and strongly interact with the P-loop residues, while the carboxyl on the pyrazoline interacts with K364 and K366 at the entrance of the active site. Considering the inherent standard errors associated with the calculated binding energy in AutoDock4.01, it's difficult to distinguish which mode is more preferable based purely on the calculated binding energies.

Molecular dynamics (MD) simulation combined with MM-PBSA/GBSA (Molecular Mechanics - Poisson-Boltzmann Surface Area/Generalized Born Surface Area) has proved to be a reliable method for investigating protein-ligand interaction and discriminating different binding modes.[43,44] Therefore 10-ns MD simulations were performed on the complex structures of binding mode **I** and **II** respectively. The Root-Mean-Square deviation (RMSD) of backbone atoms of the protein and heavy atoms of **C21** were calculated with respect to the initial coordinates (Fig. 3a). The backbone atoms in both binding modes showed almost identical and stable RMSD of ~0.9 Å, indicating that the protein had no obvious conformation changes during the MD simulations. In contrast, the RMSD of **C21** in mode **II** quickly reached the plateau (2.1 ± 0.3 Å), while that in mode **I** achieved the higher plateau (3.5 ± 0.5 Å) after 0.5 ns. Both RMSDs indicated that shifts, but the lower plateau in mode **II** suggested that the initial conformation and position of **C21** were better kept, supporting the notion that mode **II** was more stable and preferable than **I**.

Binding free energies from MM-GBSA calculation were used to further discriminate the two binding modes from the energy perspective. Based on 1,800 snapshots extracted from the MD trajectories between 1 and 10 ns at a time interval of 5 ps, the total binding free energy and individual components were calculated (Table 2). The significantly more negative total binding free energy ($\Delta G_{MM\text{-}GBSA}$, −63.60 *vs.* −36.54) in mode **II** provided further evidence that mode **II** was more preferable. In detail, the preferred binding came from a remarkable favorable electrostatic interactions (−693.69 *vs.* −669.36) and a slightly favorable van der Waals interactions (−26.67 *vs.* −23.26), while the polar and non-polar components of solvation free energy were almost identical in both binding modes.

To get a better understanding of the energy profile, the total binding free energy was decomposed into pairwise residue interaction. Sixteen residues with interaction energy less than - **C21** underwent remarkable conformation changes and/or position 0.50 kcal/mol in mode **II** were shown in Fig. 3b. It was clear that residues in the P-loop provided the most contribution to the binding, with R465 contributing ~20% and other P-loop residues (H458 to G464) contributing ~57%. Two residues K366 and K364, located at the entrance of active site pocket, contributed another ~20%. As shown in Fig. 2c, the two SO_3^- groups interacted with the P-loop residues through seven H-bonds, three of them from the first SO_3^- with ε-N

and η-N of R465 and the backbone N of S460, and the other four from the second SO_3^- with the backbone N of A461, G464, R465 and γ-O of S460. At the same time, all P-loop residues as well as Q506, Q510 and Y279 were within 5 Å distance of **C21**, resulting in abundant van der Waals interactions. These H-bond and van der Waals interactions tied the benzene moiety at the active site and contribute to ~80% total binding free energy. On the other side, the carboxyl group made H-bonds with the ζ-N of K366 and K364, as well as the long range electrostatic interactions with R362; the pyrazoline moiety also made van der Waals interactions with these three residues. Thus the interactions from pyrazoline moiety further enhanced the binding affinity of **C21** with SHP2.

Mapping the residues interacting with **C21** onto the amino acid sequence of SHP2 and making alignment with SHP1 and PTP1B (Fig. 4), we found that almost all contact residues were conserved among these three enzymes except for R362 and K364, suggesting that the region around these two residues might contribute to the selectivity of **C21** over PTP1B and SHP1. Since K364 is unique to SHP2 (Fig. 4) and contributes more binding free energy than R362 (Fig. 3b), we studied two SHP2 mutants bearing substitutions at residue K364, which corresponds to an Arg in SHP1 and a Ser in PTP1B. **C21** was 3-fold less active against SHP2/K364R (IC_{50} = 26 μM) and 7-fold less active against SHP2/K364S (IC_{50} = 56 μM) as compared to the wild type SHP2. In fact, the IC_{50} values for SHP2/K364R and SHP2/K364S approach those observed for SHP1 and PTP1B. These results are consistent with the predictions from molecular modeling indicating that K364 is indeed involved in binding **C21** and contributes to the selectivity of SHP2 for compound **C21**. Although the rest of the contact residues are the same for SHP2, SHP1, and PTP1B (Fig. 4), their immediate neighboring residues and residues that form the second shell of the **C21** binding pocket are different (the sequence identities among the three PTPs are 40–50%). These structural differences will result in non-identical **C21** binding pocket and likely also contribute to the specificity of **C21** for SHP2. Further structural study of the complexes of **C21** with SHP2 and/or PTP1B/SHP1 will be required to fully understand the determinants for **C21** recognition.

Other than identifying the interaction residues in SHP2 from docking and mutagenesis studies, we also sought to identify the key interaction points in **C21** through classical structure-activity relationship (SAR) investigation so as to guide future optimizations. Four analogues of **C21** were purchased and evaluated for inhibitory activity against SHP2 (Table 1). Compound **C21-A1**, lacking the SO_3^- group at position 1 (namely 1-SO_3^-), showed ~5-fold decreased inhibition (IC_{50} = 41 μM). By removing the 4-CH_3 from **C21-A1**, the affinity of compound **C21-A2** for SHP2 further decreased ~4-fold (IC_{50} = 155 μM). When the 2-SO_3^- in **C21-A2** was removed or the 4'-COO^- in **C21-A1** was replaced with methyl, the resulting **C21-A3** or **C21-A4** failed to inhibit SHP2 at 1 mM compound concentration. These SAR results indicated that: (1) The simultaneous presence of the 2-SO_3^- and 4'-COO^- at both sides is essential for SHP2 inhibition, and the lack of either negatively-charged center will abolish the binding affinity. (2) Both the 1-SO_3^- and 4-CH_3 groups contribute to SHP2 binding, and together they enhance the inhibitory activity about 20-fold (**C21** *vs.* **C21-A2**). These findings also agree well with the proposed binding mode **II** (Fig. 2b and 2c): the two negatively-charged centers on the two rings in **C21** simultaneously interact with the two positively-charged sites in SHP2 (the active site and a peripheral site defined by residues K364 and K366) through six H-bonds (four from 2-SO_3^- and two from 4'-COO^-), which precisely position **C21** at the active pocket. Then the 1-SO_3^- (additional 3 H-bonds with the P-loop) and 4-CH_3 (hydrophobic interaction with Y279) further enhance the binding affinity and increase the inhibition potency.

In summary, we identified a novel SHP2 inhibitor (**C21**) with micromolar inhibition potency (K_i = 4.6 μM) and good selectivity against a panel of mammalian PTPs. Through molecular

docking, MD simulation and MM-GBSA binding free energy calculation, a most likely binding mode was proposed and subsequently validated from both the receptor (mutagenesis study) and ligand (SAR study) perspectives. Our study provided a novel scaffold upon which more potent and selective SHP2 inhibitors could be developed through structural modifications, such as extending the 4-CH_3 to hydrophobic chains for more interactions with the pTyr-loop; substituting the 2'-carbonyl with bulky and hydrophobic groups to complement the free space around the WPD-loop; replacing the sulfonic groups with trifluoromethyl or trifluoromethyl sulfonyl to improve the cell permeability without total loss of electronegativity at this site. The current structure-based drug discovery approach, involving multiple computational techniques, classical inhibition analysis, site-directed mutagenesis and SAR study, should also be applicable to the identification of small molecule inhibitors for other PTPs.

Supplementary Material

Refer to Web version on PubMed Central for supplementary material.

Acknowledgments

The virtual screenings, MD simulations and MM-GBSA calculations were carried out on the BigRed supercomputer in Indiana University. This work was supported in part by National Institutes of Health Grants CA126937 and CA152194.

References and notes

1. Hunter T. Philos. Trans. R. Soc. Lond. Ser. B-Biol. Sci. 1998; 353:583. [PubMed: 9602534]
2. Tonks NK, Neel BG. Curr. Opin. Cell Biol. 2001; 13:182. [PubMed: 11248552]
3. Zhang ZY. Curr. Opin. Chem. Biol. 2001; 5:416. [PubMed: 11470605]
4. Tonks NK. Nat. Rev. Mol. Cell Biol. 2006; 7:833. [PubMed: 17057753]
5. Ventura JJ, Nebreda AR. Clin Transl Oncol. 2006; 8:153. [PubMed: 16648114]
6. Ostman A, Hellberg C, Bohmer FD. Nat. Rev. Cancer. 2006; 6:307. [PubMed: 16557282]
7. Tautz L, Pellecchia M, Mustelin T. Expert Opin. Ther. Targets. 2006; 10:157. [PubMed: 16441235]
8. Scott LM, Lawrence HR, Sebti SM, Lawrence NJ, Wu J. Curr. Pharm. Design. 2010; 16:1843.
9. Jiang ZX, Zhang ZY. Cancer Metastasis Rev. 2008; 27:263. [PubMed: 18259840]
10. Blaskovich MAT. Curr. Med. Chem. 2009; 16:2095. [PubMed: 19519384]
11. Vintonyak VV, Antonchick AP, Rauh D, Waldmann H. Curr. Opin. Chem. Biol. 2009; 13:272. [PubMed: 19410499]
12. Deb TB, Wong L, Salomon DS, Zhou GC, Dixon JE, Gutkind JS, Thompson SA, Johnson GR. J. Biol. Chem. 1998; 273:16643. [PubMed: 9642214]
13. Qu CK. Biochim. Biophys. Acta-Mol. Cell Res. 2002; 1592:297.
14. Neel BG, Gu HH, Pao L. Trends Biochem.Sci. 2003; 28:284. [PubMed: 12826400]
15. Dance M, Montagner A, Salles JP, Yart A, Raynal P. Cell. Signal. 2008; 20:453. [PubMed: 17993263]
16. Tartaglia M, Mehler EL, Goldberg R, Zampino G, Brunner HG, Kremer H, van der Burgt I, Crosby AH, Ion A, Jeffery S, Kalidas K, Patton MA, Kucherlapati RS, Gelb BD. Nature Genet. 2001; 29:465. [PubMed: 11704759]
17. Zenker M, Buheitel G, Rauch R, Koenig R, Bosse K, Kress W, Tietze HU, Doerr HG, Hofbeck M, Singer H, Reis A, Rauch A. J. Pediatr. 2004; 144:368. [PubMed: 15001945]
18. Tartaglia M, Gelb BD. Annu. Rev. Genomics Hum. Genet. 2005; 6:45. [PubMed: 16124853]
19. Tartaglia M, Niemeyer CM, Fragale A, Song XL, Buechner J, Jung A, Hahlen K, Hasle H, Licht JD, Gelb BD. Nature Genet. 2003; 34:148. [PubMed: 12717436]
20. Bentires-Alj M, Paez JG, David FS, Keilhack H, Halmos B, Naoki K, Maris JM, Richardson A, Bardelli A, Sugarbaker DJ, Richards WG, Du JY, Girard L, Minna JD, Loh ML, Fisher DE,

Velculescu VE, Vogelstein B, Meyerson M, Sellers WR, Neel BG. Cancer Res. 2004; 64:8816. [PubMed: 15604238]

21. Loh ML, Reynolds MG, Vattikuti S, Gerbing RB, Alonzo TA, Carlson E, Cheng JW, Lee CM, Lange BJ, Meshinchi S. Leukemia. 2004; 18:1831. [PubMed: 15385933]
22. Loh ML, Vattikuti S, Schubbert S, Reynolds MG, Carlson E, Lieuw KH, Cheng JW, Lee CM, Stokoe D, Bonifas JM, Curtiss NP, Gotlib J, Meshinchi S, Le Beau MM, Emanuel PD, Shannon KM. Blood. 2004; 103:2325. [PubMed: 14644997]
23. Chan G, Kalaitzidis D, Neel BG. Cancer Metastasis Rev. 2008; 27:179. [PubMed: 18286234]
24. Miyamoto D, Miyamoto M, Takahashi A, Yomogita Y, Higashi H, Kondo S, Hatakeyama M. Oncogene. 2008; 27:3508. [PubMed: 18223690]
25. Hatakeyama M. Nat. Rev. Cancer. 2004; 4:688. [PubMed: 15343275]
26. Chen LW, Sung SS, Yip MLR, Lawrence HR, Ren Y, Guida WC, Sebti SM, Lawrence NJ, Wu J. Mol. Pharmacol. 2006; 70:562. [PubMed: 16717135]
27. Noren-Muller A, Reis-Correa I, Prinz H, Rosenbaum C, Saxena K, Schwalbe HJ, Vestweber D, Cagna G, Schunk S, Schwarz O, Schiewe H, Waldmann H. Proc. Natl. Acad. Sci. U. S. A. 2006; 103:10606. [PubMed: 16809424]
28. Geronikaki A, Eleftheriou P, Vicini P, Alam I, Dixit A, Saxena AK. J. Med. Chem. 2008; 51:5221. [PubMed: 18702480]
29. Hellmuth K, Grosskopf S, Lum CT, Wurtele M, Roder N, von Kries JP, Rosario M, Rademann J, Birchmeier W. Proc. Natl. Acad. Sci. U. S. A. 2008; 105:7275. [PubMed: 18480264]
30. Lawrence HR, Pireddu R, Chen LW, Luo YT, Sung SS, Szymanski AM, Yip MLR, Guida WC, Sebti SM, Wu J, Lawrence NJ. J. Med. Chem. 2008; 51:4948. [PubMed: 18680359]
31. Yu WM, Guvench O, MacKerell AD, Qu CK. J. Med. Chem. 2008; 51:7396. [PubMed: 19007293]
32. Wu D, Pang Y, Ke Y, Yu J, He Z, Tautz L, Mustelin T, Ding S, Huang Z, Feng GS. PLoS One. 2009; 4:e4914. [PubMed: 19290061]
33. Chen LW, Pernazza D, Scott LM, Lawrence HR, Ren YA, Luo YT, Wu X, Sung SS, Guida WC, Sebti SM, Lawrence NJ, Wu J. Biochem. Pharmacol. 2010; 80:801. [PubMed: 20510203]
34. Scott LM, Chen L, Daniel KG, Brooks WH, Guida WC, Lawrence HR, Sebti SM, Lawrence NJ, Wu J. Bioorg Med Chem Lett. 2010; 21:730. [PubMed: 21193311]
35. Zhang X, He YT, Liu SJ, Yu ZH, Jiang ZX, Yang ZY, Dong YS, Nabinger SC, Wu L, Gunawan AM, Wang LN, Chan RJ, Zhang ZY. J. Med. Chem. 2010; 53:2482. [PubMed: 20170098]
36. Zhang S, Zhang ZY. Drug Discov. Today. 2007; 12:373. [PubMed: 17467573]
37. Irwin JJ, Shoichet BK. J. Chem Inf. Model. 2005; 45:177. [PubMed: 15667143]
38. Barr AJ, Ugochukwu E, Lee WH, King ONF, Filippakopoulos P, Alfano I, Savitsky P, Burgess-Brown NA, Muller S, Knapp S. Cell. 2009; 136:352. [PubMed: 19167335]
39. Moustakas DT, Lang PT, Pegg S, Pettersen E, Kuntz ID, Brooijmans N, Rizzo RC. J. Comput.-Aided Mol. Des. 2006; 20:601. [PubMed: 17149653]
40. Lang PT, Brozell SR, Mukherjee S, Pettersen EF, Meng EC, Thomas V, Rizzo RC, Case DA, James TL, Kuntz ID. RNA-Publ. RNA Soc. 2009; 15:1219.
41. Morris GM, Goodsell DS, Halliday RS, Huey R, Hart WE, Belew RK, Olson AJ. J. Comput. Chem. 1998; 19:1639.
42. Huey R, Morris GM, Olson AJ, Goodsell DS. J. Comput. Chem. 2007; 28:1145. [PubMed: 17274016]
43. Kollman PA, Massova I, Reyes C, Kuhn B, Huo SH, Chong L, Lee M, Lee T, Duan Y, Wang W, Donini O, Cieplak P, Srinivasan J, Case DA, Cheatham TE. Accounts Chem. Res. 2000; 33:889.
44. Wang JM, Morin P, Wang W, Kollman PA. J. Am. Chem. Soc. 2001; 123:5221. [PubMed: 11457384]

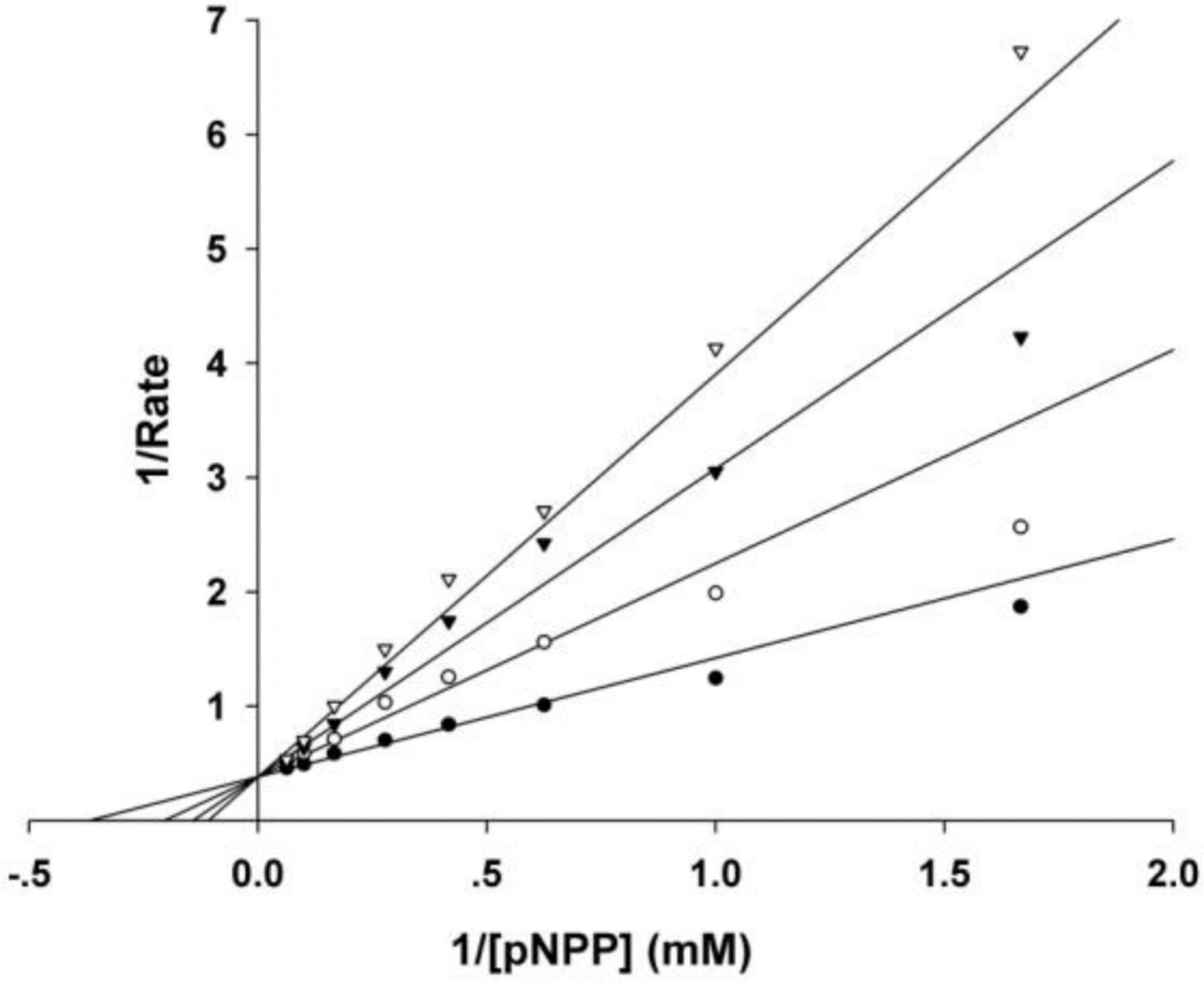

Figure 1.
Kinetic analysis of **C21** mediated SHP2 inhibition showed a competitive inhibition mode. The concentrations of **C21** were 0 (●), 4 (○), 8 (▼) and 12 μM (▽) respectively.

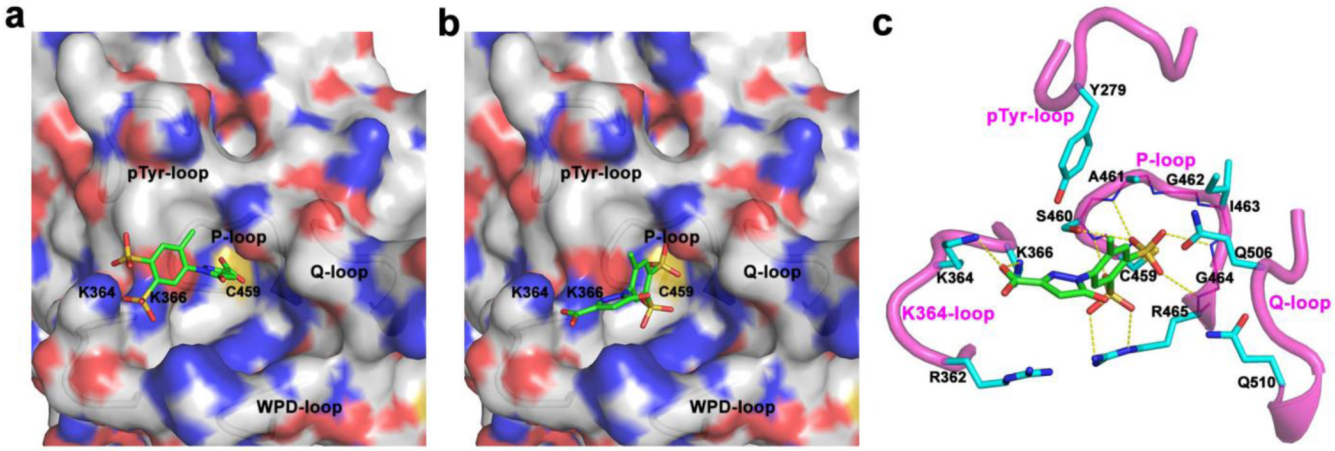

Figure 2.

Binding mode **I** a) and mode **II** b) revealed by molecular docking. c) Interaction details of **C21** and SHP2 in binding mode **II**. **C21** (green carbon) and residues within 5 Å distance of **C21** (cyan carbon) are presented in stick; H-bond interactions are highlighted in yellow dash line.

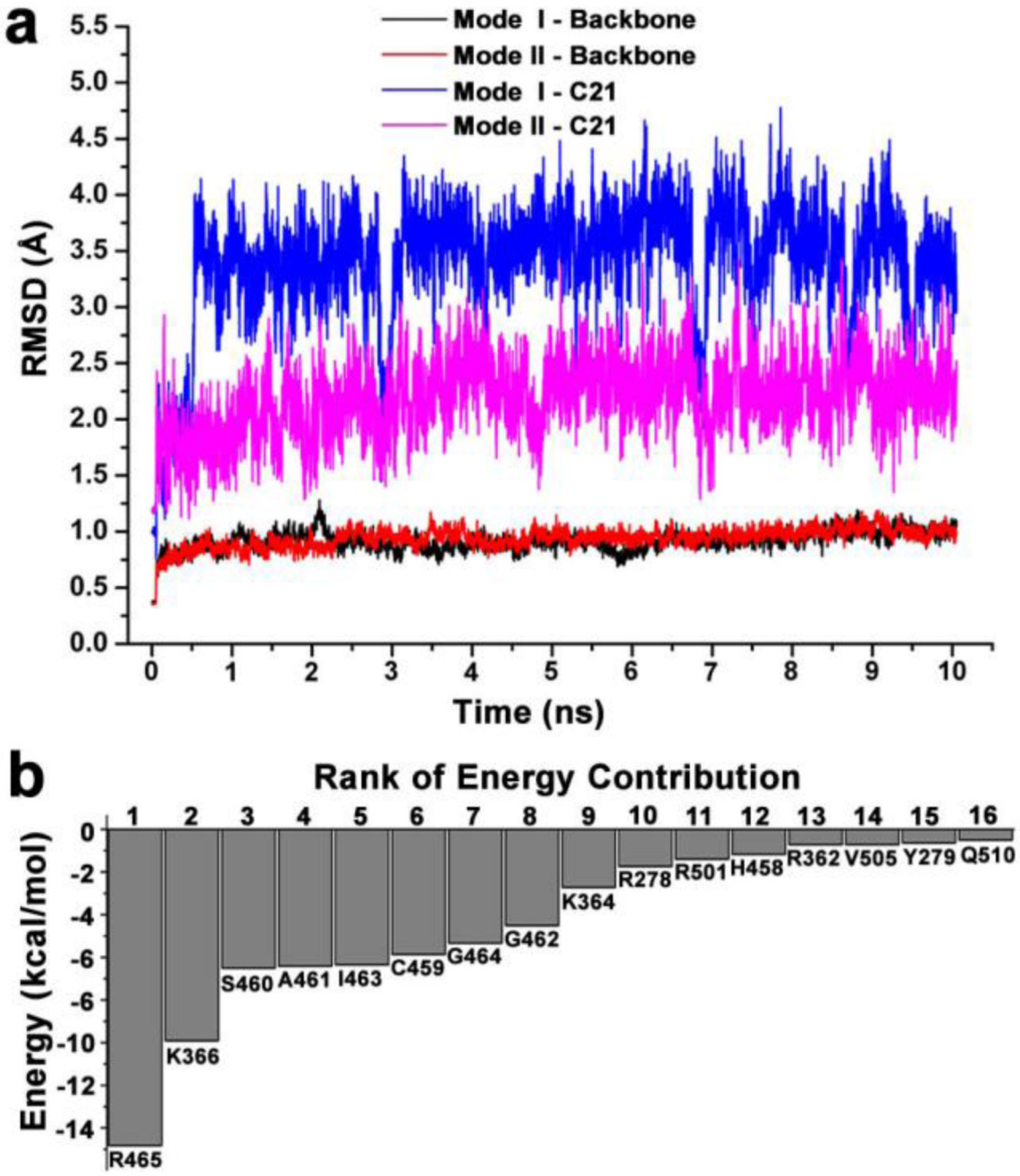

Figure 3.

a) The RMSD of backbone atoms of SHP2 protein and heavy atoms of **C21**. b) The top sixteen pairwise residue interaction energies in mode **II**.

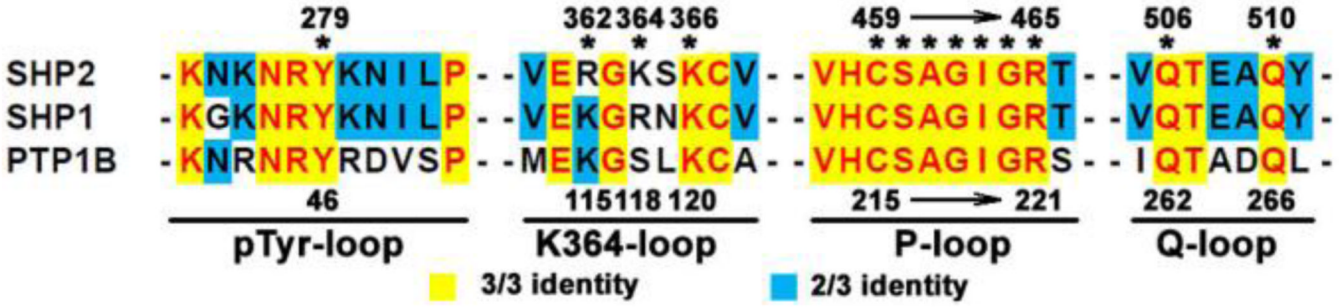

Figure 4.

Sequence alignment of four segments of SHP2 interacting with **C21**. Residue numbers in SHP2 and PTP1B are labeled at the top and bottom, respectively. Residues within 5 Å of **C21** in binding mode **II** are marked by *.

Table 1

Structures and IC_{50} values of **C18**, **C21**, **C30**, and four analogues of **C21** against SHP2.

Compd.	Structure	IC_{50} (μM)
C18	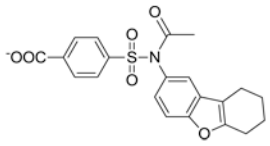	181 ± 12
C30	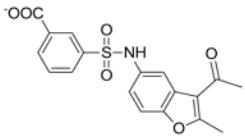	176 ± 11
C21	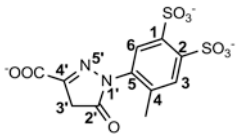	8.3 ± 0.1
C21-A1	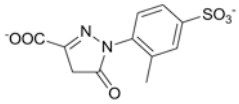	41 ± 1
C21-A2	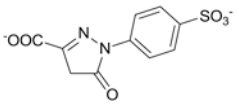	155 ± 6
C21-A3	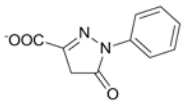	ND[a]
C21-A4	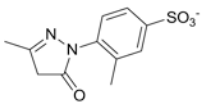	ND[a]

[a] No detectable inhibition at 1,000 μM

Table 2

The calculated binding free energies and individual energy components (kcal/mol) for binding mode **I** and **II**.

Mode	ΔE_{VDW}[a]	ΔE_{ELE}[b]	ΔE_P[c]	ΔG_{NP}[d]	$\Delta G_{MM\text{-}GBSA}$[e]
I	−23.26±0.08	−669.36±1.01	660.59±0.93	−4.51±0.01	−36.54±0.13
II	−26.67±0.09	−693.69±0.91	660.87±0.84	−4.12±0.01	−63.60±0.15

[a] Van der Waals interaction energy in gas phase.

[b] Electrostatic interaction energy in gas phase.

[c] Polar component in solvation free energy.

[d] Non-polar component in solvation free energy.

[e] Total binding free energy.